

05,10

To an analytical theory of higher-order magnetic skyrmions in nonuniform magnetic fields

© M.S. Shustin¹, D.M. Dzebisashvili¹, V.A. Stepanenko²

¹Kirensky Institute of Physics, Federal Research Center KSC SB, Russian Academy of Sciences, Krasnoyarsk, Russia

²Siberian Federal University, Krasnoyarsk, Russia

E-mail: mshustin@yandex.ru

Received April 17, 2023

Revised April 17, 2023

Accepted May 11, 2023

It is shown that axially symmetric inhomogeneous magnetic fields can lead to stabilization of higher-order magnetic skyrmions with topological charge $|Q| > 1$ due to orbital effects. We developed the analytical theory on the energy, size, and domain wall width of the such skyrmions in a power-law inhomogeneous fields, with a parameters corresponding to strongly correlated electron systems. The results obtained may have applications in describing the formation of nontrivial magnetic structures in inhomogeneous fields of superconducting vortices in heterostructures superconductor — chiral magnet of the type $[\text{Ir}_1\text{Fe}_{0.5}\text{Co}_{0.5}\text{Pt}_1]^{10}/\text{MgO}/\text{Nb}$.

Keywords: magnetic skyrmions, nonuniform magnetic fields.

DOI: 10.21883/PSS.2023.06.56111.41H

1. Introduction

Skyrmions are topologically non-trivial field configurations that are solutions to non-linear differential equations of physics. Such solutions were obtained by Skyrme in nuclear physics for baryon field [1,2]. Similar field distributions $\mathbf{m}(\mathbf{r})$ were later found in magnetic systems [3–8]. Thus, for 2D magnetic skyrmions defined by a classical field $\mathbf{m}(\mathbf{r})$, a topological charge may be introduced [9]:

$$Q = \frac{1}{4\pi} \int_{-\infty}^{\infty} \int_{-\infty}^{\infty} \left(\mathbf{m} \cdot \left[\frac{\partial \mathbf{m}}{\partial x} \times \frac{\partial \mathbf{m}}{\partial y} \right] \right) dx dy, \quad (1)$$

such that structures with different Q cannot be deformed into to each other without overcoming the energy barrier: infinite in continuous approximation (if $\mathbf{m}(\mathbf{r})$ is a continuous function) and finite allowing for discrete magnetic moment distribution. Geometrical meaning of Q is in how many „times“ vector \mathbf{m} sweeps under mapping $S^2 \rightarrow S^2$. Obviously, for a homogeneous magnetic state $Q = 0$, while for the magnetic skyrmion (MS) $Q = \pm 1$ (see below). The foregoing provides so-called topological stability of skyrmions states and causes interest in such structures as promising objects for creation of next generation logic and memory devices [10–14].

Until recently, the majority of investigations of topological magnetic structures has been devoted to 2D-MS with $|Q| = 1$. However, over the last years, more exotic magnetic excitations such as, for example, skyrmioniums, skyrmion bags, etc., attract extensive interest [15–21]. So-called 2D higher-order magnetic skyrmions (HOMS) with magnetization azimuthal angle (vorticity) $\phi = n\varphi$, where

φ is the polar angle in the film plane, will be investigated herein. Whereby $|n| > 1$ meets $|Q| = |n| > 1$. At this point, HOMS have been much less studied compared with MS. This is due to the fact that Dzyaloshinski–Moriya interaction has no contribution to the HOMS energy. Considering this, several models have been proposed where HOMS resulted from frustrated exchange interaction [15–17]. However, such mechanism requires fine selection of magnetic materials and has no necessary flexibility to vary HOMS properties which is suitable for practical applications.

A new formation mechanism for 2D-HOMS based on the influence of orbital effects of nonuniform magnetic field has been proposed by us recently [22]. From magnetic point of view, the orbital effects of magnetic field result in the occurrence of a so-called scalar chiral or three-spin interaction [23–29], which is, for homogeneous field, proportional to the density of topological magnetic configuration charge and may result in new structures in inhomogeneous fields [22]. It should be also noted that the contribution of scalar chiral interaction to energy of the MS with $n = 1$ in strongly correlated electronic systems may be comparable with the Dzyaloshinski–Moriya interaction contribution for 2D skyrmions. For HOMS with $n > 1$, the Dzyaloshinski–Moriya contribution is equal to zero and magnetic nontrivial states are stabilized due to scalar chiral interaction.

It is important that the study of magnetic skyrmions in nonuniform magnetic fields has currently got additional significance in terms of investigation of magnetic skyrmion — superconducting vortex (SV) bound states [30–36]. Thus, it has been recently experimentally found that such pairs, MS–SV, may form bound states in

[Ir₁Fe_{0.5}Co_{0.5}Pt₁]¹⁰/MgO/Nb heterostructures [33]. Moreover, it has been theoretically shown that the stray fields of superconducting vortex may be one of the stabilization factors of the axially symmetrical MS–SV structure [34–36]. In the latter case, the HOMS situation in the axially symmetrical magnetic field, studied herein, may be fulfilled. The MS (HOMS)–SV bound states themselves may carry the Majorana zero modes, having good prospects in quantum computations [37–39].

Taking into account the foregoing, it seems important to study the implementation conditions and main HOMS properties (energy, radius, domain wall width and topological charge) in axially symmetric inhomogeneous magnetic fields with various radial profiles $B(r)$. Such analysis has been carried out in our recent work within the variational approach for special cases of $B(r) \sim r, 1/r$ [22]. Herein, we generalize the analytical theory describing HOMS in the fields with arbitrary power-law functions of field $B(r) \sim r^\beta$ (arbitrary β). An important aspect of constructing a theory is the use of a hierarchy of magnetic energy parameters corresponding to strongly correlated electronic systems. For solution of the variational equations, mathematical tools of the theory of functions of many complex variables were used [40,41]. This allowed to describe analytically nontrivial dependences of HOMS size on the strength of the applied magnetic field and to find a nontrivial competition between orbital and Zeeman magnetic field contributions during stabilization of such structures. The found effects may be useful for experimental or numerical search of HOMS. Moreover, we believe that the proposed approach for analytical description of HOMS may be used to study other magnetic excitations such as skyrmioniums, bimerons, skyrmion bags, etc.

2. Energy functional and HOMS implementation conditions in inhomogeneous fields

We will study the conditions for the HOMS realization within the framework of the following energy functional describing the energy of the magnetic system

$$\begin{aligned} \mathcal{H} = & - \sum_{\langle f,g \rangle} \mathcal{J} \cdot \mathbf{S}_f \cdot \mathbf{S}_g + \sum_{\langle f,g,l \rangle \in \Delta} \mathcal{K} \cdot \mathbf{S}_f \cdot [\mathbf{S}_g \times \mathbf{S}_l] \\ & - \mathcal{B} \sum_f S_f^z - \mathcal{A} \sum_f (S_f^z)^2. \end{aligned} \quad (2)$$

The first term in the right-hand part describes the exchange interaction between sites f and g being the nearest neighbors (symbol $\langle f, g \rangle$) with amplitude $\mathcal{J} > 0$. The second term describes the three-spin interaction between three nearest neighbors f, g and h with amplitude \mathcal{K} . $\mathcal{A} > 0$ describes the „easy axis“ single-ion anisotropy, \mathcal{B} is the external magnetic field strength along the z axis expressed in energy units. The z axis is assumed to be

orthogonal to the 2D plane of the system, in which the moments \mathbf{S}_r , which are considered to be classical three-component vectors, are localized. The described interactions are competing: exchange (\mathcal{J}), anisotropic (\mathcal{A}), and Zeeman (\mathcal{B}) interactions form the tendency of magnetic moments to align collinearly with respect to each other and the z axis, while the scalar chiral interaction tends to form non-collinear magnetic configurations. Type of magnetic structures and excitations is determined by the ratio of the amplitudes of these parameters. In this work, we will use the following parameter hierarchy

$$\mathcal{J} \gg \mathcal{K} \gg \mathcal{A}, \mathcal{B}, \quad (3)$$

which takes place when considering layered strongly correlated systems [22–28]. It is important that microscopic origin of scalar chiral interaction is related to orbital magnetic field effects. In continuous approximation, such interaction amplitude \mathcal{K} may be assumed to follow the external magnetic field profile: $\mathcal{K}(r) \sim \mathcal{B}(r)$. In case of a homogeneous field, $\mathcal{B}(r) = \text{const}$, the scalar chiral interaction contribution is proportional to topological charge Q and cannot induce new magnetic configurations. It will be shown below that consideration of the external magnetic field inhomogeneity results in the situation when scalar chiral interaction can stabilize both 2D MS with $n = 1$ as well as the HOMS with $n > 1$. It should be also noted that functional (2) does not include the vector chiral interaction or Dzyaloshinski–Moriya one which is typically used to describe the MS. However, it can be easily shown that consideration of the Dzyaloshinski–Moriya interaction will change the results of the predicted theory only for MS with $n = 1$ and will not affect the results for HOMS with $n > 1$ in any way [22]. Thus, the orbital effects of inhomogeneous magnetic field will serve below as a single MS and HOMS formation mechanism.

HOMS stabilization in the inhomogeneous field will be addressed using a variational approach for a continuous version of the classical functional (2). A two-parameter ansatz will be used as a function describing HOMS formation [42]:

$$\begin{aligned} m_x &= \sin \Theta \cos n\varphi; \quad m_y = \sin \Theta \sin n\varphi; \quad m_z = \cos \Theta; \\ \Theta(r, R, w) &= 2 \arctan \left(\frac{\cosh(R/w)}{\sinh(r/w)} \right) \\ &\sim 2 \arctan \left(e^{(R-r)/w} \right) + 2 \arctan \left(e^{(-R-r)/w} \right). \end{aligned}$$

Such parametrization has a meaning of axially symmetrical 1D domain wall, where w is the width, R is the distance from the skyrmion center to the domain wall middle. All distances will be defined in terms interatomic spacing — a . Vorticity n for skyrmions is assumed larger than zero in modulus, while $|n| = |Q|$. The spatial profile visualization of MS with $n = 1$ and HOMS with $n = 2$ built using (4) is shown in Figure 1. The axis of rotation of the axially symmetrical magnetic field profile is assumed hereinafter to

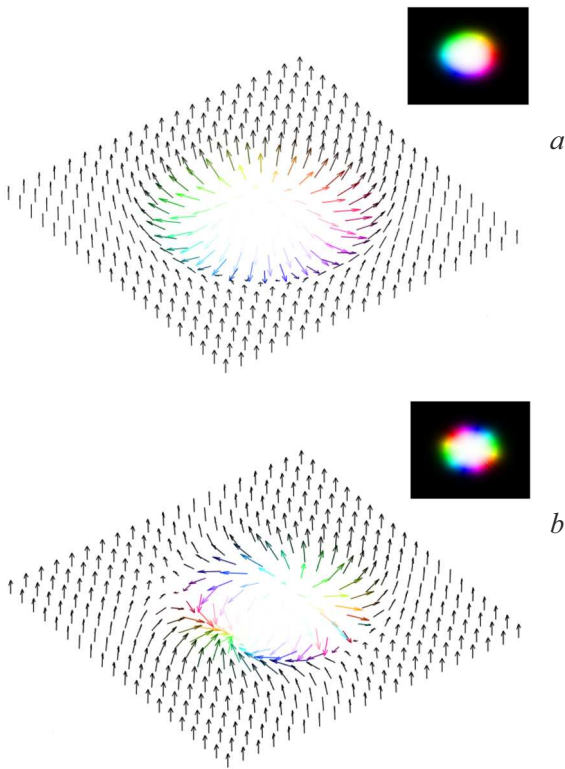


Figure 1. Spatial profiles: *a*) MS with $n = 1$, *b*) HOMS with $n = 2$. The right-hand inserts show profile visualization through a color scheme used below. Black and white color correspond to directions with $m_z = \pm 1$, respectively. In case of $m_z \neq 1$, the color corresponds to the direction of magnetization field projection $\mathbf{m}(\mathbf{r})$ on the XoY plane. If $\{m_x, m_y\} = \{1, 0\}$, then color is red; $\{m_x, m_y\} = \{\cos 2\pi/3, \sin 2\pi/3\}$ is green; $\{m_x, m_y\} = \{\cos 4\pi/3, \sin 4\pi/3\}$ is blue. For clarity, profiles $\mathbf{m}(\mathbf{r})$ are represented using the same color code.

go through the skyrmion center (point $r = 0$) perpendicular to the film plane. It will be also assumed that, among the (meta) stable configurations of functional (2), skyrmions with narrow domain wall, $R \gg w$, are implemented. This assumption is justified by the following calculations. Under this assumption, we write approximately

$$\Theta(r, R, w) \cong 2 \arctan \left(e^{(R-r)/w} \right). \quad (4)$$

Note that for profile (4), the following relations are met

$$\begin{aligned} \frac{d\Theta}{dr} &= -2f(r-R); \quad \sin \Theta = 2wf(r-R); \\ 1 - \cos \Theta &= 2n_F \left(\frac{r-R}{w} \right), \end{aligned} \quad (5)$$

where $n_F \left(\frac{r-R}{w} \right)$ is the Fermi–Dirac function, and function $f(r-R)$ is written as

$$f(r-R) = \frac{1}{R} \frac{R}{w} \frac{e^{(r-R)/w}}{1 + e^{2(r-R)/w}}.$$

With $R/w \gg 1$, function $f(r-R)$ is localized in the vicinity of point $r = R$, is symmetrical and has a constant area. The same is true of $f^2(r-R)$. Therefore, within $R/w \rightarrow \infty$, they may be approximated by delta functions

$$\begin{aligned} \lim_{R/w \rightarrow \infty} f(r-R) &\rightarrow \frac{\pi}{2} \delta(r-R), \\ \lim_{R/w \rightarrow \infty} f^2(r-R) &\rightarrow \frac{1}{2w} \delta(r-R). \end{aligned} \quad (6)$$

Finally, we will make an assumption about the functional dependence of the axially symmetric profile of the external magnetic field: we will assume that it is described by a piecewise function of the following form:

$$\mathcal{B}(r) = \begin{cases} 0, & r < \delta r \ll 1 \\ r^\beta, & r \geq \delta r, \quad \beta \in \mathbb{R} \end{cases}, \quad (7)$$

whereby the equal-zero condition of the magnetic field strength at $r < \delta r$ allows to address profiles with $\beta < 0$. Then, proceeding to the continuous description in a standard way, we find the approximate dependences of the partial contributions to the energy functional of the HOMS on its parameters

$$E_J = \frac{J}{2} \int_0^\infty \left[\left(\frac{d\Theta}{dr} \right)^2 + \frac{\sin^2 \Theta}{r^2} \right] r dr \cong J (\rho + n^2 \rho^{-1}), \quad (8)$$

$$E_A = \frac{A}{2} \int_0^\infty \sin^2 \Theta r dr \cong A \rho w^2 \quad (9)$$

$$E_K = \frac{Kn}{2} \int_0^\infty r^\beta \sin \Theta \frac{d\Theta}{dr} dr \cong -Kn \rho^\beta w^\beta, \quad (10)$$

$$\begin{aligned} E_Z &= \frac{H}{2} \int_0^\infty r^\beta (1 - \cos \Theta) r dr \\ &\cong -H \left(\frac{w}{2} \right)^{\beta+2} \Gamma_{\beta+2} \text{Li}_{\beta+2} (\delta r, -e^{2\rho}). \end{aligned} \quad (11)$$

Here, variable $\rho = R/w$ was introduced in the right-hand part, and $\rho, w \gg 1$ is assumed below. The right-hand parts of expressions (8)–(11) were calculated using relations (4)–(6). For this, integral connection between Fermi function $n_F(r/w - \rho) \sim 1 - \cos \Theta$ and incomplete polylogarithm $\text{Li}_{\beta+2}(\delta r, -e^{2\rho})$ was used:

$$\begin{aligned} \text{Li}_\beta (\delta r, -e^{2\rho}) &= \sum_{k=1}^\infty (-1)^k \frac{e^{2k\rho}}{k^\beta} \frac{\Gamma(\beta, k\delta r)}{\Gamma(\beta)} \\ &= \frac{-1}{\Gamma_\beta} \int_{\delta r}^\infty \frac{t^{\beta-1} dt}{e^{t-2\rho} + 1}, \end{aligned} \quad (12)$$

where definition of an incomplete gamma-function with variable lower limit was used

$$\Gamma(\beta, k\delta r) = \int_{k\delta r}^{\infty} t^{\beta-1} e^{-t} dt. \quad (13)$$

It is obvious that at $\delta r = 0$ the incomplete polylogarithm is reduced to a standard polylogarithm, $\text{Li}_{\beta+2}(\delta r = 0, -e^{2\rho}) = \text{Li}_{\beta+2}(-e^{2\rho})$. Energy parameters J , A , K and H in (8)–(11) are proportional to \mathcal{J} , \mathcal{A} , \mathcal{K} and \mathcal{B} in (2), respectively. The coefficients of proportionality depend on the geometry and lattice constants as well as on the magnetoactive ion spins. Herein, parameters in (8)–(11) will be assumed as independent, but hierarchy

$$J \gg K \gg A, H, \quad (14)$$

derived from that described above (3) will be used. Considering the foregoing, the dependence of the excitation energy on the size of the HOMS can be written in the form

$$E = E_J + E_K + E_A + E_Z = J(\rho + n^2\rho^{-1}) - Kn\rho^\beta w^\beta + A\rho w^2 - H\left(\frac{w}{2}\right)^{\beta+2} \Gamma_{\beta+2} \text{Li}_{\beta+2}(\delta r, -e^{2\rho}). \quad (15)$$

Minimization of functional (15) requires solving a system of nonlinear equations for ρ and w . The analytical search for such a solution in general terms is a complex mathematical problem. However, taking into account the hierarchy of energy parameters (14) makes it possible to carry out a qualitative, but simplified, description of the system, which makes it possible to develop the analytical theory of HOMS. Thus, taking into account only the term with the parameter J in (15) leads to the appearance of a line, $\rho = n$, of degenerate local minima in the (ρ, w) plane. Since J is the largest energy parameter, let us consider the behavior of functional (15) along the given line

$$E \rightarrow \tilde{E}(w) = E(w, \rho = n). \quad (16)$$

In such approximation, the search for a local minimum meeting HOMS is limited to the search for a minimum for one-variable function $\tilde{E}(w)$. Possibility of such description is shown in Figure 2. Then to assess the typical HOMS dimensions, the following equation (provided that $w \gg 1$ and $d^2\tilde{E}/dw^2 > 0$) shall be solved:

$$\frac{1}{w} \frac{d\tilde{E}}{dw} = 2An - K\beta n^{\beta+1} w^{\beta-2} - H \frac{\beta+2}{2\beta+1} \Gamma_{\beta+2} \text{Li}_{\beta+2}(\delta r, -e^{2n}) w^\beta = 0. \quad (17)$$

Solution of equation (17) with $H \neq 0$ will be described in the next paragraph. Here, HOMS properties with only orbital field effects present will be discussed briefly. Such situation may take place in case of zero values of g -factors

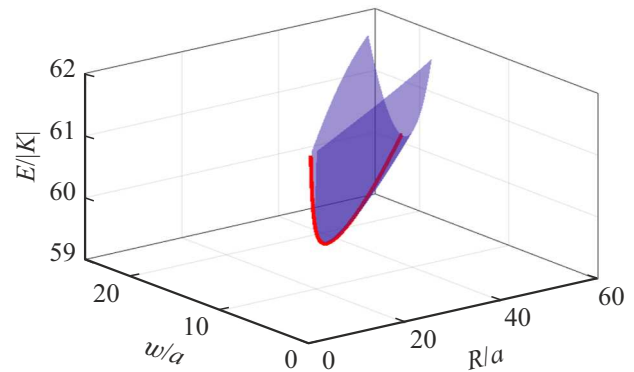


Figure 2. Energy surface section of $E(R, w)$ (16) with $n = 3$ in variables $R = \rho w$ and w . Thick line — behavior of $\tilde{E}(w)$ (18) along line $R = nw$. It can be seen that minimum points $E(R, w)$ and $\tilde{E}(w)$ coincide and, therefore, a simplified description using one-variable function $\tilde{E}(w)$ may be used to find them. The following energy parameters are chosen: $J = 10$, $K = -1$, $H = -0.006$, $A = 0.001$.

of magnetoactive ions. Then, it is easy to show that higher-order skyrmion dimensions are defined by expressions

$$w_* = \left(\frac{Kn^\beta}{2A}\right)^{\frac{1}{2-\beta}}, \quad R_* = nw_*,$$

$$\beta < 2; \quad \text{sign}(Kn^\beta) = \text{sign}(\beta A); \quad \text{sign}(An) > 0. \quad (18)$$

In particular, in the physically interesting case when the skyrmion is in the superconducting Pearl vortex field, $B(r) = 1/r$ ($\beta = -1$) may be approximated [30–32], the given relations are written as

$$w_* = \sqrt[3]{\frac{|K|}{2An}}; \quad R_* = nw_*; \quad K < 0.$$

Since the sign of constant K is defined by the magnetic flux sign, HOMS formation due to the orbital effects of an inhomogeneous field may be possible only with a certain direction of the latter. Thus, it can be seen from (18) that for „ascending“ fields ($\beta > 0$), the external field shall be co-directional to the magnetic moment of the ferromagnetic film. While for „decreased“ fields ($\beta < 0$), the situation is inversed and an external field shall be applied opposite to the initial film magnetization direction in order to form HOMS. As will be shown below, these features are also maintained in a qualitative sense when the Zeeman effects of magnetic field are considered.

3. Analytical description of HOMS in the case of $H \neq 0$

HOMS stabilization conditions considering both Zeeman and orbital magnetic field contributions to the energy of 2D magnetic system will be described below. First, qualitative aspects of the competition of terms in (17) with

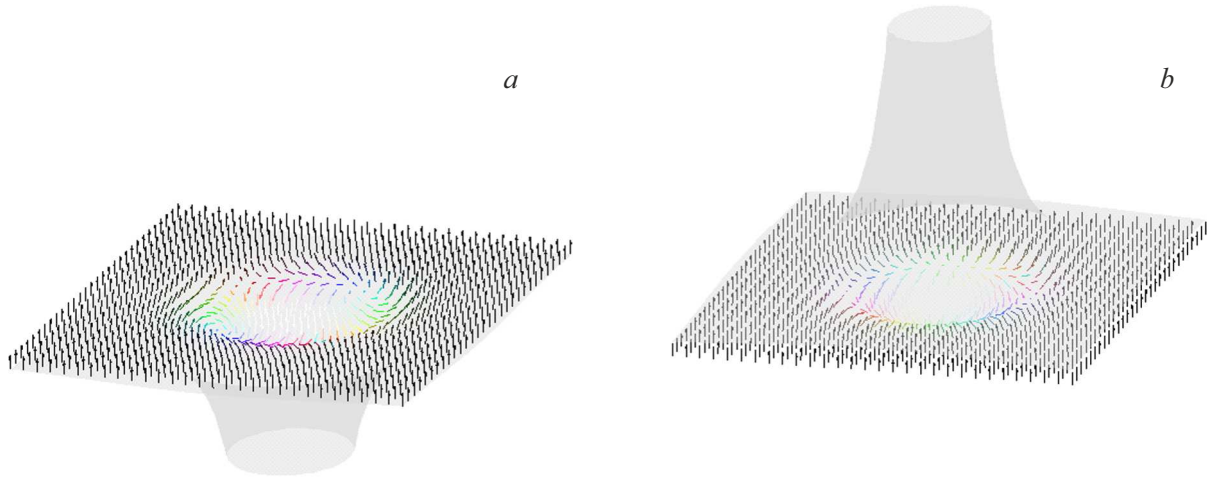


Figure 3. Visualization of HOMS spatial profiles in an inhomogeneous „linearly descending“ field $B(R) = 1/r$ ($\beta = -1$). Cases *a*) and *b*) correspond to the situations when the field is applied along the film saturation magnetization and in opposite direction: such configurations are stable and nonstable, respectively.

$H \neq 0$ will be discussed. For this, it is convenient to discuss behavior of equation (17) separately for positive, $\beta > 0$, and negative, $\beta = -\alpha < 0$, degrees of field profile $\mathcal{B}(r)$. For the latter, a new variable $m = 1/w$ will be introduced. The equations for the functional minimum will be written as

$$\begin{aligned} \frac{1}{w} \frac{d\tilde{E}}{dw} &= -K\beta n^{\beta+1} w^{\beta-2} + H(2+\beta)v_{\beta} w^{\beta} \\ &+ 2An = 0; \quad \beta > 0 \end{aligned} \quad (19)$$

$$\begin{aligned} m^3 \frac{d\tilde{E}}{dm} &= -Kan^{1-\alpha} m^{\alpha+2} - H(2-\alpha)v_{\alpha} m^{\alpha} \\ &- 2An = 0; \quad \alpha > 0. \end{aligned} \quad (20)$$

The following parameters are introduced here

$$\begin{aligned} v_{\beta} &= -\frac{\Gamma_{2+\beta}}{2^{1+\beta}} \text{Li}_{2+\beta}(\delta r, -e^{2n}) > 0, \\ v_{\alpha} &= -\frac{\Gamma_{2-\alpha}}{2^{1-\alpha}} \text{Li}_{2-\alpha}(\delta r, -e^{2n}) > 0. \end{aligned} \quad (21)$$

To the solutions w_* and m_* of Eqs. (19) and (20) should be subjected to the conditions for minimizing the functional, as well as limiting the range of their values based on the previously used assumptions about the narrowness of the domain wall of the HOMS

$$\left. \frac{d^2\tilde{E}}{dw^2} \right|_{w=w_*} > 0; \quad w_* \gg 1; \quad \left. \frac{d^2\tilde{E}}{dm^2} \right|_{m=m_*} > 0; \quad 0 < m_* \ll 1.$$

This means that the right-hand parts of equations (19) and (20) shall go through zero with the sign changed from negative to positive like functions w and m , respectively. For equation (19), such solution is achieved, if $\text{sign}(K) = \text{sign}(H) = 1$. In this case, with sufficiently

low w , the second term in the right-hand part (17) dominates, because $Kw^{\beta-2} \gg Hw^{\beta}$. With sufficiently high w , the inequality is inverted and function $d\tilde{E}/dw$ changes sign in point $w_* \gg 1$. High values w_* are related to condition $K \gg H$. Thus, as a result of consideration of the Zeeman effects of skyrmion interaction with the „increased“ magnetic field ($\beta > 0$), HOMS formation conditions are not restricted by conditions $\beta < 2$ any longer, as was the case with only orbital effects of magnetic field (see equation (18)).

In case of „decreased“ magnetic fields, $\alpha > 0$, competition of orbital (K) and Zeeman (H) magnetic field effects in expression (20) differs for $\alpha < 2$ and $\alpha \geq 2$. For $\alpha < 2$, $v_{\alpha} \sim n^{2-\alpha}$, and therefore, in the actual searching range, we have

$$|Kan^{1-\alpha} m^{\alpha+2}| \sim |H(2-\alpha)v_{\alpha} m^{\alpha}|;$$

$$0 < m \ll 1; \quad 0 < \alpha < 2.$$

The latter means that search for physical solutions of $m_* \ll 1$ is more preferable, if constants K and H are of the same sign. Moreover, since at $m = 0$, the right-hand part of equation (20) is $-2An$, then the optimal way of finding of physical solution corresponding to the HOMS is to fulfil relations

$$\text{sign}(An) = 1, \quad \text{sign}(K) = \text{sign}(H) = -1.$$

Thus, in case of „moderately decreasing“ fields (7) with $-2 < \beta < 0$, HOMS can be also implemented essentially. However, unlike $\beta > 0$, the external magnetic field shall be applied in the direction opposite to ferromagnetic ordering of the initially magnetized film.

Examples of stable and nonstable HOMS configurations with $n = 2$ and field profile $\mathcal{B}(r) = 1/r$ ($\alpha = 1$) are shown in Figure 3. Thus, Figure 3, *a*) shows stable configuration when magnetic field is directed opposite to the film

magnetization vector beyond the HOMS localization region meeting relations (27). Figure 3, *b* shows a similar, but nonstable configuration when the field is directed along the film saturation magnetization. This difference is caused by the fact that for the case *a* the Zeeman contribution to the HOMS excitation energy $E_Z < 0$ and stabilizes the nontrivial configuration, because the field strength near the skyrmion core is maximum and the moments are oriented along the field. For the case *b*, the Zeeman contribution results in HOMS destabilization due to positive E_Z .

In case of rather fast decreasing fields, $\alpha > 2$, partial contribution to the Zeeman term in equation (20) increases faster compared with orbital contribution: function v_α increases with α . Moreover, the Zeeman sign changes compared with $\alpha < 2$.

This leads to the fact that, in the case of $\alpha \gg 1$, the stabilization of the HOMS is also possible, and this is mainly due to the Zeeman effects of the magnetic field, the direction of which can be codirectional with the direction of the film magnetization.

Considering the foregoing, qualitative aspects of competition between different energy contributions during formation of stable HOMS with sharp domain wall may be summarised using the stability diagram shown in Figure 4. The diagram was plotted taking into account that energy parameter hierarchy (15) meeting the strongly correlated electronic systems is implemented. In addition, since K and H describe the orbital and Zeeman contributions into the energy of excitation/magnetic field interaction, respectively, $\text{sign}(K) = \text{sign}(H)$ was assumed. Region „1“ in Figure 4 meets the condition when only orbital effects of the magnetic field contribute to the HOMS energy: $H = 0$. In this case, as mentioned in the end of Section 2, HOMS are formed with $\beta < 2$ and other relations of constitutive parameters as given in (20). Region „2“ meets the ascending magnetic fields taking into account the Zeeman effects of magnetic field. As mentioned above (see the discussion under equation (25)), competition between orbital and Zeeman magnetic field effects is such that HOMS with sharp domain wall may occur almost with any field degrees and strengths H . The latter is represented by the fact that region „2“ occupies almost the whole quadrant of the coordinate axes as shown in Figure 4. Regions „3“ in Figure 4 corresponds to the situation of descending magnetic fields ($\beta < 0$) having their maximum near the HOMS center. In this case, for HOMS stabilization, the applied external magnetic field shall be negative, i.e. directed opposite to the film saturation magnetization. Moreover, if $\text{sign}(K) = \text{sign}(H)$ is assumed, then the foregoing means that HOMS in the descending fields will certainly stabilize, if $-2 < \beta < 0$. But if $\beta < -2$, then from equation (23), it follows that the Zeeman and orbital contributions will become competitive and HOMS stabilization will become more problematic and, in case of $-2\beta \gg 2$, impossible. Such feature is qualitatively shown in Figure 4 in the form of filled region „3“ that occupies a part of the third quadrant of variables β, H .

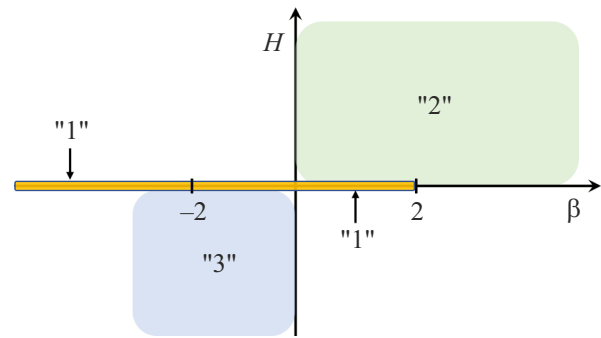


Figure 4. Quantitative diagram of HOMS stability in variables: magnetic field profile exponent β (see equation (6)), amplitude H of applied external magnetic field at distance $r = a$ from the skyrmion center. Energy parameter hierarchy (15) and $\text{sign}(H) = \text{sign}(K)$ are assumed to be implemented. Regions „1“, „2“ and „3“ correspond to the HOMS stability regions and are described by relations: (20); $H > 0, \beta > 0$; (27), respectively. In the latter case, β is assumed to be not much lower than -2 .

Having discussed the qualitative effects of competition of various energy contributions to equations (19) and (20), solution of these equations will be provided. „Decreased“ fields will be investigated i.e. equation (20) will be solved. Equation for „increased“ fields (19) can be solved in the similar way. The simplest case $\alpha = 1$ will be discussed first. This corresponds to radial decreased magnetic field according to $\mathcal{B}(r) = 1/r$, that is implemented, for example, in the superconducting vortex field. In this case, equation (20) for stabilization of higher-order skyrmion size is reduced to

$$Km^3 + 2Hnm + 2An = 0. \tag{22}$$

Analytical expression for the HOMS domain wall width is easily derived from this equation:

$$w_* = \frac{u^{1/3}}{u^{2/3} - Hn/3K};$$

$$u = \left| \frac{An}{K} \right| \left(\sqrt{1 + \left(\frac{H}{3} \right)^3 \frac{An}{K}} - \text{sign} \left(\frac{An}{K} \right) \right).$$

Behavior of w_* (23) and $R_* = w_*n$ is illustrated in Figure 2 as functions of applied external magnetic field $|H|$ for HOMS with various topological charges n . It can be seen that the domain wall width increases with increasing $|H|$ and decreases with increasing n . The optimum HOMS radius increases as function of $|H|$, and n .

It may be useful in practice to represent solution of equation (22) as a series in a small parameter. For hierarchy (14) discussed herein, such expansion may be written as [43]:

$$m_* = \frac{1}{w_*} = \frac{1}{3} \sum_{j=0}^{\infty} \frac{(-1)^j}{j!} \frac{\Gamma \left(\frac{j+1}{3} \right)}{\Gamma \left(\frac{4-2j}{3} \right)} \left(\frac{H}{\sqrt[3]{KA^2/2n}} \right)^j. \tag{24}$$

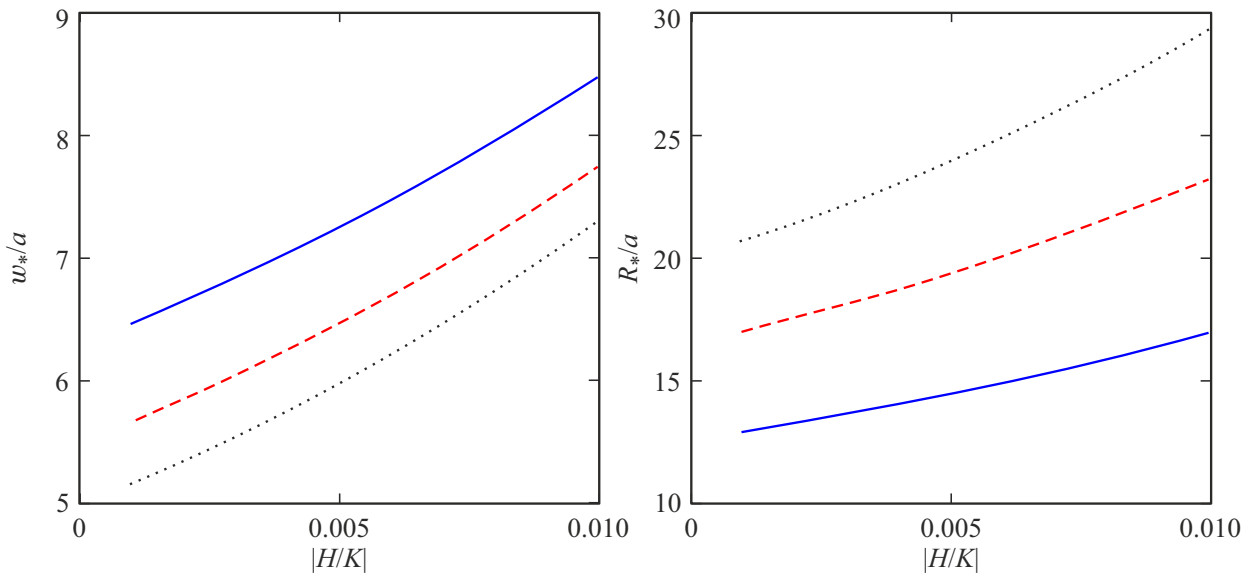


Figure 5. Dependences of the optimum domain wall width w_* (left) and radius R_* (right) on the external magnetic field strength at $\beta = -\alpha = -1$. System parameters are the same as shown in Figure 1. Solid, dashed and dotted curves correspond to HOMS with $n = 2, 3, 4$, respectively.

Generally (arbitrary α), equation (20) is not solvable by radicals. However, similar to (24), it may be expressed as a series in a small parameter. For this, consider the case when the field descending degree is represented in the form of a rational fraction $\alpha = p/q$ ($p, q > 0$). This assumption is rather general, because irrational α may be approximated by rational fractions with arbitrary preassigned accuracy. Then, equation (20) may be written as

$$a = l^p \cdot (1 + hl^{2q}), \tag{25}$$

where

$$l = m^{1/q}, \quad a = \frac{-2An}{H(2-\alpha)v_\alpha}, \quad h = \frac{Kan^{1-\alpha}}{H(2-\alpha)v_\alpha}, \quad \alpha = p/q.$$

Equation in the form (25) may be solved using the formula [40,41]:

$$l = a^{1/p} + \sum_{\gamma=2}^{\infty} A_\gamma a^{\gamma/p};$$

$$A_\gamma = \frac{1}{\gamma!} \mathcal{D}^\gamma \left(\frac{l}{(1+h \cdot l^{2q})^{(\gamma+1)/p}} \left(l(1+h \cdot l^{2q})^{1/p} \right)' \right) \Big|_{l=0}, \tag{26}$$

where \mathcal{D}^γ denotes the operator of differentiation of multiplicity γ with respect to the variable l . Then, taking into account that $l = m^{1/q}$ and raising the series in expression (26) to power q , we obtain the expression for inverse width of the domain wall with arbitrary rational $\alpha = p/q$:

$$m_* = \sum_{k=q}^{\infty} B_k a^{k/p};$$

$$B_k = \sum_{\substack{q=\gamma_1+\dots+\gamma_k \\ \{k=1, \gamma_1+\dots+(k-q+1)\cdot\gamma_{k-q+1}\}}} \frac{q!}{\gamma_1! \dots \gamma_{k-q+1}!} A_1^{\gamma_1} \dots A_{k-q+1}^{\gamma_{k-q+1}}. \tag{27}$$

Functions A_γ may be calculated using the binomial formula

$$\frac{\mathcal{D}^\gamma}{\gamma!} (F \cdot G_\gamma) \Big|_{l=0} = \sum_{k=0}^{\gamma} \frac{1}{k!(\gamma-k)!} \left[\frac{d^k F(l)}{dl^k} \cdot \frac{d^{\gamma-k} G_\gamma(l)}{dl^{\gamma-k}} \right] \Big|_{l=0},$$

where functions

$$F(l) = l \left(l(1+h \cdot l^{2q})^{1/p} \right)'_l,$$

$$G_\gamma(l) = (1+h \cdot l^{2q})^{-(\gamma+1)/p}$$

are introduced in expression (26). n -th order derivative of complex function $G_\kappa = g^{-\kappa}$, where $g = 1 + h \cdot l^{2q}$ and $\kappa = (\gamma + 1)/p$, may be calculated using the Faa di Bruno formula:

$$\frac{d^n G_\kappa}{dl^n} = \sum_{k=1}^n \sum_{\substack{k=\alpha_1+\dots+\alpha_n \\ \{n=1\alpha_1+\dots+n\alpha_n\}}} \frac{n!}{\alpha_1! \dots \alpha_n!} \times \left(\frac{d^k g^{-\kappa}}{dk^k} \right) \left(\frac{1}{l!} \frac{dg}{dl} \right)^{\alpha_1} \dots \left(\frac{1}{n!} \frac{d^n g}{dl^n} \right)^{\alpha_n}, \tag{28}$$

which completes the solution of Eq. (19) for rational α .

Finally, it should be noted that the found solutions (24) and (27) written as series by the parameters of equation (20) describe the inverse width of the HOMS domain wall, $m_* = 1/w_*$. At the same time, presentation in the form of similar expansions of w_* may be useful. For this purpose, a useful equation will be given here to derive the coefficients of expansion into series which is multiplicative

inverse to the initial series. Suppose the initial series is given here

$$b_0 + b_1x + b_2x^2 + b_3x^3 + \dots$$

with known coefficients b_0, b_1 etc. Then to find the multiplicative inverse series,

$$\frac{1}{b_0 + b_1x + b_2x^2 + b_3x^3 + \dots} = c_0 + c_1x + c_2x^2 + c_3x^3 + \dots,$$

coefficients c_0, c_1 , etc., shall be found. It may be shown that the latter may be found using the following relations:

$$c_0 = \frac{1}{b_0}, \quad c_k = \frac{(-1)^k}{b_0^{k+1}} \Delta_k,$$

where Δ_k designates determinants from matrices composed of the coefficients from the initial series written as follows:

$$\Delta_k = \begin{vmatrix} b_1 & b_2 & b_3 & \dots & \dots & b_{k-1} & b_k \\ b_0 & b_1 & b_2 & \dots & \dots & b_{k-2} & b_{k-1} \\ 0 & b_0 & b_1 & \dots & \dots & b_{k-3} & b_{k-2} \\ 0 & 0 & b_0 & \dots & \dots & b_{k-4} & b_{k-3} \\ 0 & 0 & 0 & \dots & \dots & b_{k-5} & b_{k-4} \\ \vdots & \vdots & \vdots & \dots & \dots & \vdots & \vdots \\ 0 & 0 & 0 & \dots & \dots & b_0 & b_1 \end{vmatrix}.$$

Then, choosing the coefficients of series (24) or the ratios of the coefficients B_{q+k}/B_q appearing in series (27) as the coefficients b_k , we can obtain an explicit form of the dependences w_* on the parameters of the right-hand sides of equations (19) and (20).

4. Conclusion

The study investigates the conditions for formation of higher-order magnetic skyrmions (HOMS) in two-dimensional systems — special-form magnetic excitations whose azimuthal magnetization angle $\phi = n\varphi$, where φ is the polar coordinate angle in the film plane, and topological charge $|Q| = |n|$. In this case, competition of exchange interaction, single-ion anisotropy as well as Zeeman and orbital effects of inhomogeneous magnetic field in the magnetic subsystem is the key factor of HOMS stabilization. Occurrence of orbital effects is limited to addition of chiral terms to the magnetic subsystem Hamiltonian. Their contribution to the magnetic configuration energy depends on the spatial distribution of the topological charge density as well as on the spatial distribution of the magnetic field.

For an analytical description of the effect of stabilization of the HOMS, we studied the sizes of higher-order skyrmions in axially symmetric inhomogeneous magnetic fields of a power-law profile, for which the transverse component (perpendicular to the plane of the film) of the field $B \sim r^\beta$, where r is the distance from the center

of the skyrmion to a point in the plane. Despite the simple functional dependence, such profile describes a wide class of magnetic field configurations near HOMS, if the sizes of the latter are much smaller than the typical scales of field strength variation. Analysis of HOMS sizes is carried out using a variational approach with well proven magnetic skyrmion profile and energy parameters hierarchy (see inequalities (3) and (14)) typical for strongly correlated electronic systems. This allows to reduce the energy functional minimization problem to a variational single-variable problem describing the HOMS domain wall width. For solution of the variational equations, for general power-law profiles $\mathcal{B}(r)$, mathematical tools of the theory of functions of many complex variables are used. This allows to describe analytically nontrivial dependences of HOMS sizes on the applied magnetic field strength and to find an abundant competition between orbital and Zeeman effects of magnetic field for stabilization of such structures. Thus, it is shown that for HOMS stabilization in fields $\beta < 0$, the external field shall be directed along the film magnetization, while for fields with $\beta > 0$ it shall be in the opposite direction.

As an important special case, HOMS formation in $\mathcal{B}(r) \sim 1/r$ type axially symmetrical „decreased“ magnetic fields (case $\beta = -1$) is investigated. Investigations of skyrmions in such types of fields have become popular over the last years due to experimental detection of magnetic skyrmion — superconducting vortex (SV) bound states in $[\text{Ir}_1\text{Fe}_{0.5}\text{Co}_{0.5}\text{Pt}_1]^{10}/\text{MgO}/\text{Nb}$ heterostructures and to theoretical prediction of stabilization of such bound states owing to interaction between the skyrmion and inhomogeneous vortex field. It should be noted that the Dzyaloshinski–Moriya interaction induced, in particular, as a result of creation of the heterostructure interface is the main stabilization mechanism of MS with $n = 1$. However, in case of HOMS with $n > 1$, such interaction does not make any substantial contribution to the spin structure energy and the scalar chiral interaction may be one of the HOMS stabilization factors. The study shows that the nonuniform vortex field together with the scalar chiral interaction may cause stabilization of the higher-order magnetic skyrmions. The very existence of scalar chiral interaction as well as the used hierarchy of material parameters (3) impose conditions on magnetic candidate materials where HOMS may be formed due to the orbital effects. Thus, microscopic derivation of magnetic interactions [22] that form functional (2) with hierarchy (3) shows that the natural candidate materials are strongly correlated layered compounds where magnetic interactions occur due to indirect exchange. Such compounds may include transition 3d- and rare-earth 4f-metals [44]. However, the question of the possibility of forming nontrivial magnetic states in them is the subject of the further study.

Acknowledgments

The authors are grateful to I.S. Burmistrov, S.S. Apostolov and E.S. Andriyakhin for useful discussions.

Funding

The research was supported by „BASIS“ Foundation for Development of Theoretic Physics and Mathematics (project No. 20-1-4-25-1), grant of the President of the Russian Federation MK-4687.2022.1.2, Krasnoyarsk Mathematical Center and financed by the Ministry of Science and Higher Education of the Russian Federation (Agreement No. 075-02-2023-936).

Conflict of interest

The authors declare that they have no conflict of interest.

References

- [1] T. Skyrme. Proc. R. Soc. Lond. Ser. A **260**, 127 (1961).
- [2] T. Skyrme. Nucl. Phys. **31**, 556 (1962).
- [3] A.A. Belavin, A.M. Polyakov. Pis'ma v ZhETF **503** (1975), (1979). (in Russian).
- [4] I.E. I.E. Dzyaloshinski, B.A. Ivanov. Pis'ma v ZhETF **592** (1979), (1979). (in Russian).
- [5] A.S. Kovalev, A.M. Kosevich, K.V. Maslov. Pis'ma v ZhETF, **30**, 321 (1979). (in Russian).
- [6] A.N. Bogdanov, D.A. Yablonsky. ZhETF **95**, 178 (1989). (in Russian).
- [7] F.N. Rybakov, N.S. Kiselev, A.B. Borisov, L. Döring, C. Melcher, S. Blügel. APL Materials **10**, 111113 (2022).
- [8] K.L. Metlov. Physica D **443**, 133561 (2023).
- [9] A.S. Schwarz. Quantum Field Theory and Topology. Springer, Berlin, Heidelberg (2013).
- [10] S.-H. Yang, K.-S. Ryu, S. Parkin. Nature Nanotechnology **10**, 221 (2015).
- [11] C. Moreau-Luchaire, C. Mouta S., N. Reyren, J. Sampaio, C.A.F. Vaz, N. Van Horne, K. Bouzehouane, K. Garcia, C. Deranlot, P. Warnicke, P. Wohlhüter, J.-M. George, M. Weigand, J. Raabe, V. Cros, A. Fert. Nature Nanotechnology **11**, 444 (2016).
- [12] X. Zhang, M. Ezawa, Y. Zhou. Sci. Rep. **5**, 9400 (2015).
- [13] J. Zázvorka, F. Jakobs, D. Heinze. Nature Nanotechnology **14**, 658 (2019).
- [14] G. Yu, P. Upadhyaya, Q. Shao, H. Wu, G. Yin, X. Li, C. He, W. Jiang, X. Han, P.K. Amiri, K. Wang. Nano Lett. **17**, 261 (2017).
- [15] A. Leonov, M. Mostovoy. Nature Commun. **6**, 8275 (2015).
- [16] R. Ozawa, S. Hayami, Y. Motome. Phys. Rev. Lett. **118**, 147205 (2017).
- [17] L. Rózsa, K. Palotás, A. Deák, E. Simon, R. Yanes, L. Udvardi, L. Szunyogh, U. Nowak. Phys. Rev. B **95**, 094423 (2017).
- [18] D. Foster, C. Kind, P.J. Ackerman, J.-S.B. Tai, M.R. Dennis, I. Smalyukh. Nature Phys. **15**, 655 (2019).
- [19] F. Rybakov, N. Kiselev. Phys. Rev. B **99**, 064437 (2019).
- [20] V.M. Kuchkin, B. Barton-Singer, F.N. Rybakov, S. Blügel, B.J. Schroers, N. Kiselev. Phys. Rev. B **102**, 144422 (2020).
- [21] B. Göbel, I. Mertig, O.A. Tretiakov. Phys. Rep. **895**, 1 (2021).
- [22] M.S. Shustin, V.A. Stepanenko, D.M. Dzebisashvili. Phys. Rev. B **107**, 195428 (2023).
- [23] D. Sen, R. Chitra. Phys. Rev. B **51**, 1922 (1995).
- [24] O.I. Motrunich. Phys. Rev. B **73**, 155115 (2006).
- [25] B. Bauer, L. Cincio, B. Keller, M. Dolfi, G. Vidal, S. Trebst, A. Ludwig. Nature Commun. **5**, 5137 (2014).
- [26] Y. Zhang, Y. Sun, H. Yang, J. Železný, S.P.P. Parkin, C. Felser, B. Yan. Phys. Rev. B, **95**, 075128 (2017).
- [27] K. Komarov, D. Dzebisashvili. J. Magn. Magn. **440**, 57 (2017).
- [28] M. Malki, G.S. Uhrig. Europhys. Lett. **132**, 20003 (2020).
- [29] J. Kipp, K. Samanta, F.R. Lux, M. Merte, D. Go, J.-P. Hanke, M. Redies, F. Freimuth, S. Blügel, M. Ležaić, Y. Mokrousov. Commun. Phys. **4**, 99 (2021).
- [30] S.M. Dahir, A.F. Volkov, I.M. Eremin. Phys. Rev. Lett. **122**, 097001 (2019).
- [31] R.M. Menezes, J.F.S. Neto, C.C. de Souza Silva, M.V. Milosevic. Phys. Rev. B **100**, 014431 (2019).
- [32] S.M. Dahir, A.F. Volkov, I.M. Eremin. Phys. Rev. B **102**, 014503 (2020).
- [33] A.P. Petrović, M. Raju, X.Y. Tee, A. Louat, I. Maggio-Aprile, R.M. Menezes, M.J. Wyszyński, N.K. Duong, M. Reznikov, Ch. Renner, M.V. Milošević, C. Panagopoulos. Phys. Rev. Lett. **126**, 117205 (2021).
- [34] E. Andriyakhina, I. Burmistrov. Phys. Rev. B —bf103, **17**, 174519 (2021).
- [35] E.S. Andriyakhina, S. Apostoloff, I.S. Burmistrov. JETP Lett. **116**, 825 (2022).
- [36] S.S. Apostoloff, E.S. Andriyakhina, P.A. Vorobyev, O.A. Tretiakov, I.S. Burmistrov. arXiv:2212.08351 (2023).
- [37] G. Yang, P. Stano, J. Klinovaja, D. Loss. Phys. Rev. B **93**, 224505 (2016).
- [38] S. Rex, I. Gornyi, A. Mirlin. Phys. Rev. B **100**, 064504 (2019).
- [39] A.O. Zlotnikov, M.S. Shustin, A.D. Fedoseev. J. Sup. Nov. Magn. **34**, 3053 (2021).
- [40] L.A. Aizenberg, A.P. Yuzhakov. Integral'nye predstavleniya i vychety v mnogomernom kompleksnom analize. Nauka, Novosibirsk (1979). 368 p. (in Russian).
- [41] T.M. Sadykov, A.K. Tsikh. Gipergeometricheskie i algebraicheskie funktsii mnogikh peremennykh. Nauka, M., (2019). 408 s. (in Russian).
- [42] X. Wang, H. Yuan, M.X. Wang. Commun. Phys. **1**, 1 (2018).
- [43] H. Mellin, C.R. Acad. Sci. Paris Sér. I. Math. **172**, 658 (1927).
- [44] B.V.Yu. Irkhin, Yu.P. Irkhin. Elektronnaya struktura, korrelyatsionnye efekty i fizicheskie svoystva d- i f-perekhodnykh metallov i ikh soedineniy i ikh soedineniy RHD, M. (2008), 476 p.

Translated by Ego Translating